

A Compensator Designed for Electro-Hydraulic Servo System in Laminar State

Le ZENG^{*,**}, Jianping TAN^{*}, Jun YANG^{***}

**State Key Laboratory of High Performance Complicated Manufacturing, College of Mechanical and Electrical Engineering, Central South University, Chinalco technology building, new campus of Central South University, Yuelu District, Changsha 410083, China, E-mail: jptan@163.com*

***Changsha Aeronautical Vocational and Technical College, Tianxinqiao, Yuhua District, Hunan Province, Changsha 410124, China, E-mail: zenglewish@163.com*

****College of Engineering and Design, Hunan Normal University, College of engineering and design, Taozihu Road, Yuelu District, Changsha 410081, China, E-mail: yangcsu@126.com (Corresponding Author)*

crossref <http://dx.doi.org/10.5755/j02.mech.26023>

1. Introduction

The electro-hydraulic servo system (EHSS) is widely used in national defences, industrial equipment, construction machinery, mining machinery, metallurgy machinery, forging machinery, and robot system [1-3]. The EHSS is affected by friction, dead zone, oil compressibility, internal leakage and other factors, and has the problems of uncertain model parameters. In order to maximize the accuracy, response speed and robustness of the electro-hydraulic system, many nonlinear control methods such as adaptive control [4], robust control [5], predictive control [6, 7], feedback linearization control [8, 9], sliding mode variable structure control [10-13], intelligent control [14, 15] are applied to the hydraulic control. Literature [16] pointed out that the non-linearity of valve controlled cylinder system is mainly caused by the non-linearity of valve orifice flow, which is the square root of the pressure difference. The effect of external load force directly affects the pressure difference of the servo valve orifice, thus affecting the output of flow and the displacement speed response of hydraulic cylinder.

In order to reduce the complex calculation of the control strategy and make it used in the industrial field, more scholars use the differential pressure compensation to suppress the speed fluctuation caused by the load disturbance. In literature [17, 18], the strategy of differential pressure and flow compensation was adopted earlier so that the flow of control system and the speed of motor were not affected by the load. Yang H.Y. [19] designed flow compensation control of the valve port strategy based on PLC. Quan L., Bai Y.H. [20, 21] adopted a composite control strategy of speed feedforward and position feedback to realize the desired control performance of speed and position under different loads. In the research the submerged orifice flow equation is used to describe the flow through the valve orifice under a certain pressure difference, and the flow coefficient is taken as a constant. But when the pressure difference or the opening of the valve orifice is very small, the flow state is laminar with low Reynolds number and the flow coefficient is a non-linear variable [22]. So the submerged orifice flow equation is difficult to describe the flow with low Reynolds number. The error of the system model leads to the poor performance of load flow compensation control, especially when the system is subjected to excessive load relative to

the maximum load of the system or small target displacement. Literature [23] shows that with the increase of external load, the accuracy of the compensator designed by empirical flow equation model decreases. Because the pressure difference between of the valve port decreases with the external load increases, the flow coefficient changes, and the accuracy of flow compensation decreases.

Ferreira J. A. [24] divided the valve model into dynamic response area and static response area. The valve orifice in the small opening state has serious nonlinearity, which is the dynamic response area. This paper analysed the load flow gain and load pressure gain of the valve controlled symmetrical cylinder system in the small opening state and the large opening state, and designed the closed-loop control for the composite model. Andreas S. [25] pointed out that the flow coefficient of the valve is related to the manufacturing accuracy of the valve and the wear of the valve. In this paper, the flow characteristic of the servo valve is tested by experiment, and the flow coefficient of the valve is estimated to determine the wear and failure of the valve. From the flow characteristic curve obtained by the experiment, it can be seen that the flow characteristic of the servo valve in the small opening state is nonlinear. Borutzky W. [25] analyses the correlation of flow coefficient and Reynolds number of servo valve. When the pressure difference is small, the flow state of the servo valve port is laminar, and the flow model is quite different from the turbulent state. Pan X.D. [26] conducted flow field simulation and experimental analysis on the flow coefficient of rectangular slide valve, obtained the function relationship between flow coefficient and Reynolds number, and established a more accurate flow model of small opening state of servo valve.

In order to improve the accuracy of load flow compensation control in the electro-hydraulic servo system, this paper analyses the laminar flow and turbulent flow state of the servo valve, and studies the load flow equation in the laminar flow state with small opening or small pressure difference of the valve orifice. Based on the expected linear flow equation and the laminar flow equation, a flow compensator is designed to compensate the flow affected by pressure difference, which makes the flow characteristics linear. It can be used as an open-loop controller to resist the nonlinearity of valve and form a composite control strategy with closed-loop control strategies to improve the accuracy of the system.

2. The flow model of the servo valve

The flow state of the servo valve can be regarded as viscous incompressible flow, and the flow under a certain pressure difference can be calculated by the submerged flow calculation formula as follows:

$$Q = C_d A \sqrt{\frac{2\Delta P}{\rho}}, \quad (1)$$

where: Q is volume flow through valve orifice, m^3/s ; Δp is pressure difference of valve orifice, Pa; ρ is hydraulic oil density, kg/m^3 ; C_d is flow coefficient; A is flow area of valve orifice, m^2 . The ideal rectangular notch throttle orifice area in spool valve can be calculated as $A = \omega x_v$, where x_v is orifice opening size, m; ω is orifice area gradient.

Numerical simulation results demonstrate that the relationship between flow coefficient C_d and Reynolds number R_e of the servo valve is approximated as Eq. (2), which was researched by Borutzky, W. and Pan, X. in [26, 27].

$$C_d = C_{dt} \sqrt{\frac{R_e}{R_e + R_c}}, \quad (2)$$

where: C_{dt} is flow coefficient in turbulent state; R_c is critical Reynolds number.

The following equation can be derived from Eqs. (1) and (2).

$$Q = C_{dt} \sqrt{\frac{R_e}{R_e + R_c}} \omega x_v \sqrt{\frac{2\Delta p}{\rho}}. \quad (3)$$

The Reynolds number R_e is a dimensionless number, and can be defined by H. E. Merritt in [28].

$$R_e = \frac{d_H}{\nu} Q, \quad (4)$$

where: ν is kinematic viscosity of fluids; d_H is hydraulic diameter.

The hydraulic diameter d_H of the spool valve orifice can be defined as:

$$d_H = \frac{4A}{\lambda} = \frac{2A}{\omega + x_v}, \quad (5)$$

where: λ is wetted perimeter of the overflow surface.

The Reynolds number R_e can be obtained from Eqs. (4) and (5).

$$R_e = \frac{2Q}{\nu(\omega + x_v)}. \quad (6)$$

When the pressure difference Δp and the opening of the valve x_v is very small, even close to zero, the flow Q and the Reynolds number R_e is too small and the flow state is laminar. As the pressure difference Δp or the opening of the valve x_v increases, the Reynolds number R_e and the flow

coefficient C_d increases. When the Reynolds number R_e is much larger than the critical Reynolds number R_c , $C_{dt} \approx C_d$. The flow coefficient keeps nearly stable, and the flow pattern has negligible effect on the flow rate of the valve.

Substituting the Eq. (6) into the Eq. (3) gives a quadratic equation for the flow.

$$2Q^2 + R_c(\omega + x_v)\nu Q - \frac{4(C_{dt}\omega x_v)^2 \Delta p}{\rho} = 0. \quad (7)$$

Solving this quadratic equation and discarding the negative root, the orifice discharge Q can be obtained as:

$$Q = \frac{\sqrt{[R_c(\omega + x_v)\nu]^2 + \frac{32(C_{dt}\omega x_v)^2 \Delta p}{\rho}}}{4} - \frac{R_c(\omega + x_v)\nu}{4}. \quad (8)$$

The orifice discharge Q is approximately to $Q = C_{dt}\omega x_v \sqrt{\frac{2\Delta p}{\rho}}$ when the pressure difference Δp or the opening of the valve x_v is large enough to make the valve orifice turbulent.

3. The expected flow equation

The nonlinearity of flow increases the difficulty of the electro-hydraulic system control. If the flow gain of the servo valve is constant, the complexity of the electro-hydraulic system model and the controller can be greatly reduced under the premise of guaranteeing control performance. For this reason, the desired flow equation of the servo valve is presented as shown in Eq. (9):

$$Q = C_{dt}\omega \sqrt{\frac{2}{\rho} \left(\frac{P_S - P_R}{2} \right)^{1/2}} x_v, \quad (9)$$

where: P_S is P port pressure of the servo valve; P_R is T port pressure of the servo valve. If the P port pressure and the T

port pressure are stable, the flow gain $C_{dt}\omega \sqrt{\frac{2}{\rho} \left(\frac{P_S - P_R}{2} \right)^{1/2}}$

of the expected flow equation is constant, and the flow rate is independent of the pressure difference ΔP of the valve orifice and linear with the valve orifice opening.

4. The design of a compensation controller

To make the output flow of the servo valve close to the expected state, a compensation controller is designed to compensate the non-linear flow caused by laminar state. The orifice opening of the servo valve after compensation is set as x_v' , and the function of the orifice opening before and after compensation is set as following:

$$x_v' = f(x_v). \quad (10)$$

To make the actual output flow Q equal to the ex-

pected discharge Q' , the simultaneous (8), (9) and (10) formula. After substituting Eq. (10) into the Eq. (8) and making

$$\frac{\sqrt{[R_c(\omega + f(x_v))v]^2 + \frac{32(C_{dt}\omega f(x_v))^2 \Delta p}{\rho}}}{4} - \frac{R_c(\omega + f(x_v))v}{4} = C_{dt}\omega \sqrt{\frac{2}{\rho}} \sqrt{\frac{P_S - P_R}{2}} x_v \dots \quad (11)$$

Through simplification and solution, compensation function $f(x_v)$ is solved as following:

$$f(x_v) = \frac{\beta\gamma}{8\alpha} \left(1 + \sqrt{1 + 32 \frac{\alpha^2}{\gamma^2} + 16 \frac{\alpha}{\gamma\beta} \frac{w}{x_v}} \right) \frac{x_v}{x_{vmax}}, \quad (11)$$

where: $\alpha = C_{dt}w \sqrt{\frac{\Delta p}{\rho}}$, $\beta = \sqrt{\frac{P_S - P_R}{\Delta p}}$ and $\gamma = R_c v$.

Assuming that the current or voltage given to the servo valve is linearly related to the valve orifice opening, the percentage of the current (voltage) to the maximum current (voltage) is set as u before compensation, and u' after compensation. Percentage of input signal before compensation u can be described as:

$$u = \frac{x_v}{x_{vmax}}. \quad (12)$$

Percentage of the input signal u' after compensation can be described as:

$$u' = \frac{x_v'}{x_{vmax}}. \quad (13)$$

$$Q_L = \frac{\sqrt{[R_c(\omega + x_v)v]^2 + \frac{32(C_{dt}\omega x_v)^2 \Delta p}{\rho}}}{4} - \frac{R_c(\omega + x_v)v}{4}. \quad (16)$$

where: $\Delta p = P_S - P_1$, when $0 \leq x_v \leq L$. While, $\Delta p = P_1 - P_R$, when $-L \leq x_v < 0$. L -the maximum opening of the valve orifice.

Literature [29] studies that the flow coefficient of a throttle valve is related to the direction of fluid flow. In order to reduce the complexity of control, the influence of flow coefficient of inflow and outflow is neglected. Through the compensation control of Eq. (14), the load flow can be theoretically controlled in accordance with the expected flow equation, that is, the load flow does not change with the external load and direction of the hydraulic rod.

6. Experiment

6.1. The experimental bench

The experimental bench shown in Fig. 2 is built according to the scheme shown in Fig. 1.

The bench consists of driving circuit of the servo valve-controlled asymmetric cylinder and load circuit of the relief valve-controlled asymmetric cylinder. The external load is simulated by adjusting the overflow pressure of the relief valve, β , and the pressure difference of the

Eq. (8) and Eq. (9) equal, the following equation can be obtained:

Substituting Eqs. (13) and (14) into the Eq. (12), percentage of input signal u' after compensation can be obtained as:

$$u' = \frac{\beta\gamma}{8\alpha} \left(1 + \sqrt{1 + 32 \frac{\alpha^2}{\gamma^2} + 16 \frac{\alpha}{\gamma\beta} \frac{w}{x_{vmax}} \frac{1}{u}} \right) u. \quad (14)$$

The compensating controller is designed according to Eq. (15) to compensate the non-linear flow affected by flow pattern, so that the actual flow output of the servo valve is equal to the expected flow. Namely, the flow output of the servo valve is linear with the opening of the valve orifice.

5. Load flow model of EHSS

The diagram of EHSS is shown in Fig. 1. The load flow is the flow into or out of the rodless cavity. Specifically, it is the flow into the rodless cavity when the cylinder is in forward motion, and the flow out of the rodless cavity but when the cylinder is in reverse motion.

According to Eq. (7), the equation of the load flow of the system Q_L is described:

valve orifice can be controlled. The flow output of the valve orifice is calculated by detecting the velocity of the hydraulic cylinder.

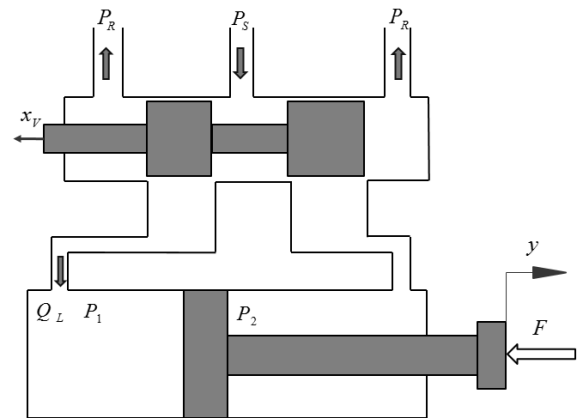


Fig. 1 The diagram of EHSS: P_1 is pressure of the rodless cavity; P_2 is pressure of the rod cavity; Q_L is the load flow; y is displacement of the rod; F is external load

The basic system parameters of the bench are shown in Table 1. According to literature [26], the value C_{dt}

is 0.61; according to the literature [31] and test, the value R_c is 170; the pressure value P_s is approximately equal to the pump outlet pressure set as 5 MPa. P_R is approximately equal to the tank pressure set as 0 MPa. P_1, P_2 is detected by the pressure sensor.

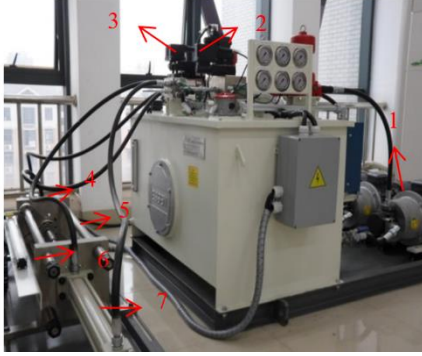


Fig. 2 The experimental bench: 1 is hydraulic pumping station; 2 is the servo valve; 3 is proportional relief valve; 4 is load cylinder; 5 is connection between top cylinder; 6 is position sensor; 7 is driving cylinder

Table 1

The basic system parameters

Parameter, Measurement unit	Value
System pressure, MPa	5
Pump speed, r/min	960
Pump displacement, ml/r	16
ρ , kg/m ³	850
Nominal flow of servo valve under differential pressure 3MPa, L/min	9
Frequency of the servo valve, Hz	100
Radius of Hydraulic cylinder, m	0.05
Rod diameter hydraulic cylinder, m	0.028
v , m ² /s	6×10^{-5}
L , m	0.5×10^{-3}
w , m	9.23×10^{-3}

6.2. Characteristics experiment of the servo valve

6.2.1. The flow characteristics of the servo valve in laminar state

When the pressure difference or the opening of the servo valve is small, the flow of the valve is laminar and in the low Reynolds state. So the test area is mainly carried out in the small opening of servo valve. In the experiment, the input signal of the valve is - 15% to 15% of the maximum rated voltage, and the signal interval is 1%. The pressure difference of the valve orifice is achieved by imposing external load to the driving cylinder. Fig. 3 shows the flow of the valve under the pressure difference of 0.5 MPa, 1.0 MPa, 1.5 MPa, 2.0 MPa, 2.5 MPa, 3.0 MPa.

The flow coefficient C_d can be obtained by transforming Eq. (1):

$$C_d = \frac{Q}{A} \sqrt{\frac{\rho}{2\Delta P}}. \quad (15)$$

According to Eq. (17) and the flow data in Fig. 3, the flow coefficient C_d of the valve is calculated as shown in Fig. 4. When the pressure difference is 0.5 MPa, and 1.0 MPa, the value of the C_d is far less than the value with

larger pressure difference. As the pressure difference increases, the difference of C_d decreases. In addition, when the valve opening is small, the C_d value is small. As the valve opening increases, the C_d value increases, approaching to constant value in the turbulent state model.

In the experiment of flow characteristics with small opening, the change of flow coefficient shows that the flow state of the valve is laminar flow when the opening and the pressure difference is small, and the flow coefficient C_d is far less than the constant value of 0.61.

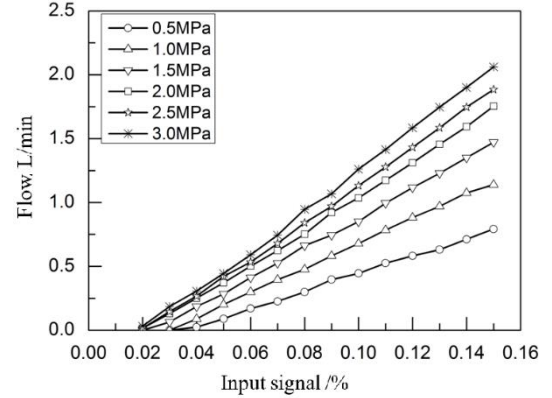


Fig. 3 The flow characteristic of the valve in laminar state

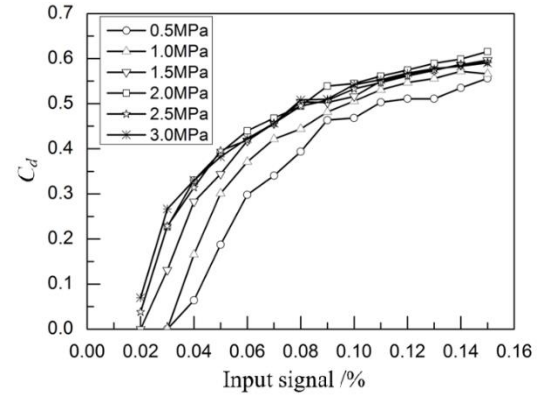


Fig. 4 The flow characteristic of the valve in laminar state

6.2.2. The flow characteristics experiment after compensation control

The pressure difference of the valve orifice varies from 0.5 MPa to 4 MPa, through imposing external load to the driving cylinder. The control system collects data of the signal input value, pressure value of two chambers and velocity of hydraulic cylinder before and after compensation control. Characteristics experiment is to verify that the compensation controller can make the flow characteristics of the servo valve close to the expected flow characteristics.

Fig. 5 shows the expected load flow curve and the load flow curve after compensation control. Through comparison, it can be seen that the load flow after compensated is linear with the valve orifice opening, and basically close to the expected load flow.

The error diagram is shown in Fig. 6. Because of the negative overlap of the servo valve at about 2%, the error is large when the orifice opening is about 1%~3%. With the increase of the orifice opening, the error decreases rapidly and is controlled within 20%. Because the flow coefficient of the valve orifice is related to the direction of the liquid

flow, the error distribution is asymmetric compared to the valve orifice opening 2%.

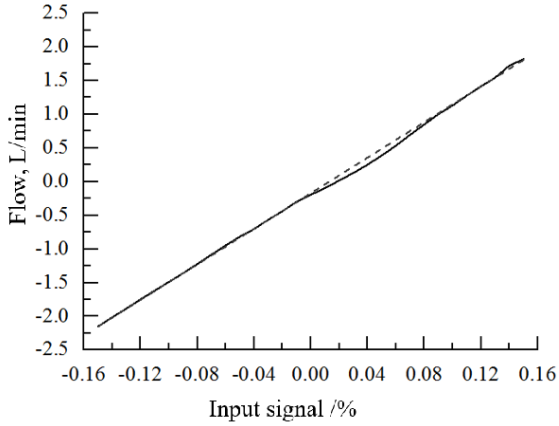


Fig. 5 The expected flow and load flow characteristic after compensation control: dash line represents the expected flow line through theoretical calculation; solid line represents the actual flow after compensated of the test bench

When the input signal is 5%, the load flow before and after compensation control is compared with the curve of pressure difference. Fig. 7 shows that the pressure difference of the valve orifice changes from 0.5 MPa to 4 MPa, and the load flow after compensation almost keeps stable which is shown in Fig. 9, while the uncompensated load flow decreases with the decrease of the pressure difference. When the pressure difference is less than 2 MPa, the load flow changes obviously with the pressure difference. In order to compensate the flow change caused by load, the compensation signal increases obviously. When the pressure difference is only 0.5 MPa, the signal input value shown in Fig. 8 after compensation control reaches about 10%. When the pressure difference is greater than 2.5 MPa, the load flow increases insignificantly, and the signal input after compensation control changes insignificantly, which decreases slightly relative to the signal of 5%.

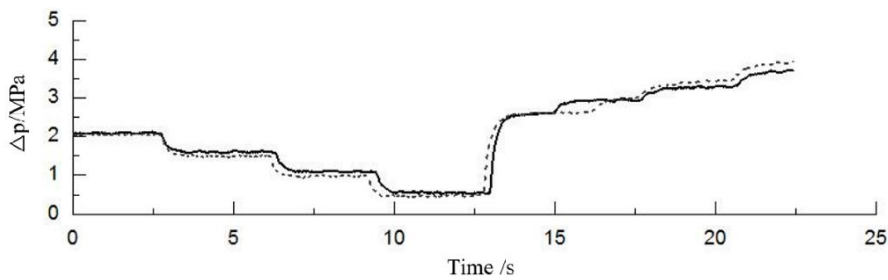


Fig. 7 The pressure difference of the valve orifice: solid line represents the pressure difference before compensation control; dash line represents the pressure difference after compensation control

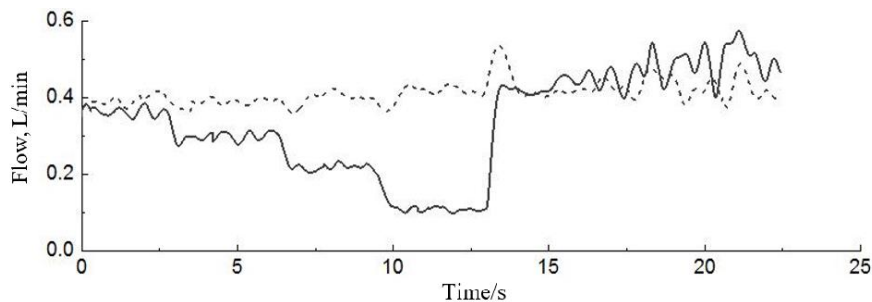


Fig. 8 The signal input to the servo valve: solid line represents the flow before compensation control; dash line represents the flow after compensation control

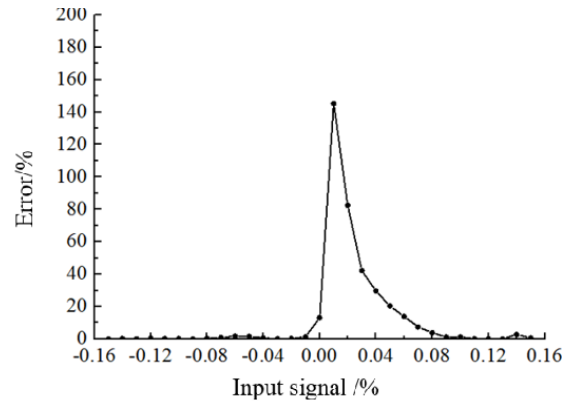


Fig. 6 Percentage error of expected load flow and load flow after compensation control

The characteristic experiment shows that when the pressure difference is small, the flow of the servo valve decreases obviously with the decrease of the pressure difference. When the pressure difference is large, the flow of the valve changes little with the pressure difference. The designed compensation controller can compensate the flow fluctuation well caused by external load, and make the flow characteristics of the servo valve approximate to the expected flow equation.

6.3. Position control experiment

6.3.1. Experimental methods and purpose

Given the sinusoidal displacement reference signal, whose amplitude is 5 mm and frequency is 0.5 Hz, the P closed-loop controller is used to test the displacement response of the EHSS with large external load. By comparing the response of the system with and without open-loop compensator, the conclusion will verify that the open-loop compensator can improve the accuracy and the anti-load interference ability with the simplest closed loop control.

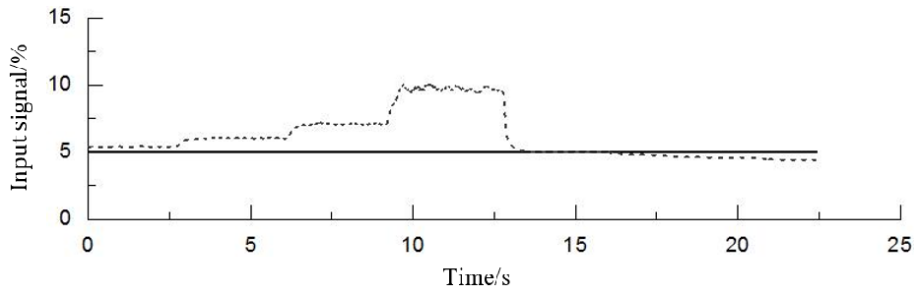


Fig. 9 The load flow through the valve orifice: solid line represents the input signal before compensation control; dash line represents the input signal after compensation control

6.3.2. Experimental results

Figs. 8-10 shows the response diagram of the system without compensation control. Fig. 8 shows the pressure variation diagram of two chambers in driving cylinder under excessive external load. The external load causes the pressure fluctuation of the rodless chamber in the driving cylinder from 2 MPa to 4.2 MPa, that is, the pressure difference of the valve orifice is 0.8 MPa to 3 MPa. Fig. 9 shows the response diagram of the cylinder tracking sinusoidal displacement signal.

Fig. 10 shows the displacement error diagram of the cylinder. From Fig. 10, it can be seen that the pressure change of the two chambers has a great influence on the motion control accuracy. When the pressure fluctuates at 2.5 MPa, that is, the pressure difference of the valve orifice is about 2.5 MPa, the maximum error is less than 5 mm. When the pressure reaches 4 MPa, that is, the pressure difference is 1 MPa, the maximum error is 0.8 mm.

Figs. 11-13 shows the system response diagram with compensator as feed control. Fig. 11 shows that the pressure of the rodless chamber in the driving cylinder fluctuates between 2 MPa and 4.2 MPa under the influence of external load, that is, the pressure difference of the valve orifice fluctuates between 0.8 MPa and 3 MPa. Figs.12 and 13 show the response diagram and error of tracking sinusoidal displacement signal of the system using compensation control. Fig. 13 shows that the displacement error of hydraulic cylinder is controlled within 0.4 mm when the pressure difference is between 0.8 MPa and 3 MPa. That is to say, compared with non-compensation control, the external load has little effect on the accuracy of the system with compensation control.

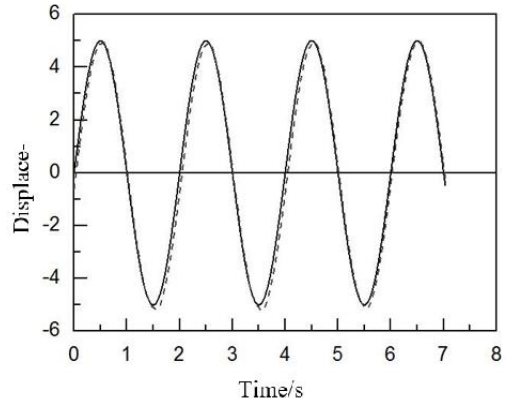


Fig. 9 Displacement response of the dive cylinder without the compensator: solid line represents the reference displacement; dash line represents the actual displacement

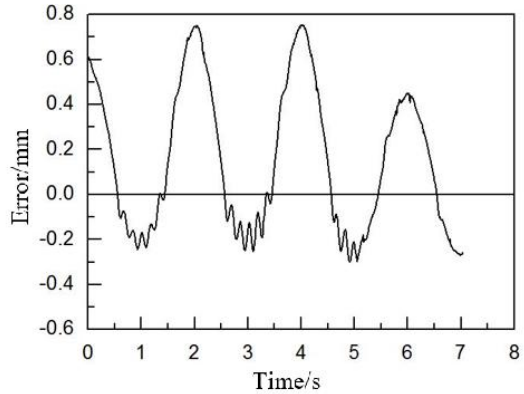


Fig. 10 The position error of the dive cylinder without the compensator

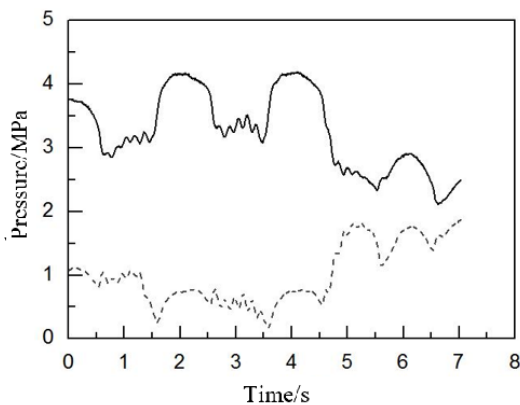


Fig. 8 The pressure variation diagram without compensation control: solid line represents the pressure in the rodless cavity; dash line represents the pressure in the rod cavity

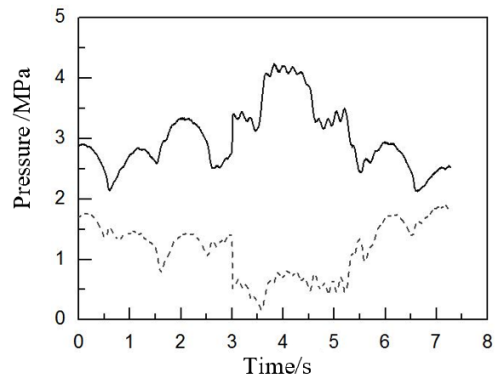


Fig. 11 The pressure diagram in experiment with compensator: solid line represents the pressure in the rodless cavity; dash line represents the pressure in the rod cavity

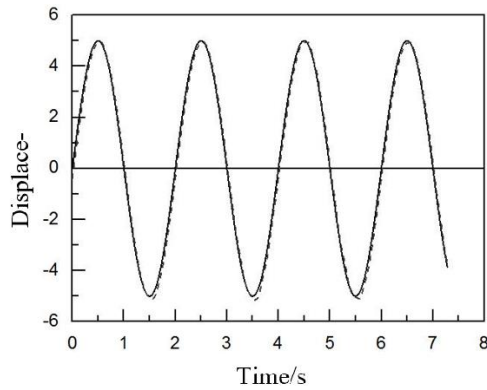


Fig. 12 The displacement of the dive cylinder with compensator: solid line represents the reference displacement; dash line represents the actual displacement

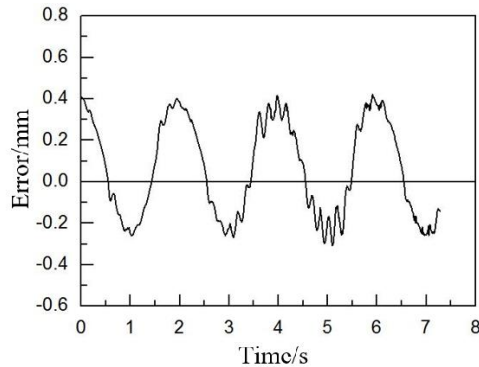


Fig. 13 The position error of the dive cylinder with compensator

Under the same control parameters, P closed loop control has realized the good motion response of EHSS tracking sinusoidal signal, whose amplitude is 5 mm and frequency is 0.5 Hz. Experiment verified that the compensator can improve the position accuracy and the anti-load interference ability of the system, with the simplest closed-loop control.

7. Conclusions

The Reynolds number is discussed which has a great influence on the flow of the valve orifice when the pressure difference and the opening of the valve is small. A novel flow equation of the valve orifice is built because the submerged flow equation cannot describe the flow accurately in the low Reynolds state. The novel flow equation is nonlinear with the orifice opening and pressure difference. The experimental results show that when the valve orifice is small or the pressure difference is small, the flow coefficient changes nonlinearly, which is far less than the constant value of 0.61. The flow state of the valve orifice is laminar with low Reynolds number.

To eliminate the nonlinear factors of the flow characteristics of the servo valve, a compensator is designed by solving the equation of the novel flow and desired flow. The characteristics experiment verified the flow curve after compensation is close to the expected flow curve.

The open-loop compensator as feed forward control compounded with the simplest proportional (P) controller are used in EHSS under heavy load relatively to system pressure. The displacement reference signal is a sinusoidal signal, whose frequency is 0.5 Hz and amplitude is 5 mm.

The experiment result shows that the compensator can greatly improve the position accuracy of the system, which the maximum error is less than 0.4 mm. While, the maximum error of the system without compensator is 0.8 mm.

By establishing feed forward compensation control of laminar flow state, the load flow nonlinearity of servo valve in extreme load state is eliminated, and the stability of the system for variable load is improved. The feed forward compensation with the simplest proportional closed-loop control can achieves a good control effect, which is suitable for industrial field control.

References

1. **Guo, K.; Wei, J.; Fang, J.;** et al. 2015. Position tracking control of electro-hydraulic single-rod actuator based on an extended disturbance observer, *Mechatronics* 27: 47-56. <http://dx.doi.org/10.1016/j.mechatronics.2015.02.003>.
2. **Xiao, L.; Lu, B.** 2015. Cascaded sliding mode force control for a single-rod electrohydraulic actuator, *Neurocomputing* 156: 117-120. <http://dx.doi.org/10.1016/j.neucom.2014.12.078>.
3. **Nguyen, M. N.; Tran, D. T.; Ahn, K. K.** 2018. Robust position and vibration control of an electrohydraulic series elastic manipulator against disturbance generated by a variable stiffness actuator, *Mechatronics* 52: 22-35. <https://doi.org/10.1016/j.mechatronics.2018.04.004>.
4. **Wang, C.; Quan, L.; Jiao, Z.** 2017. Nonlinear adaptive control of hydraulic system with observing and compensating mismatching uncertainties, *IEEE Transactions on Control Systems Technology* 1-12. <http://dx.doi.org/10.1109/TCST.2017.2699166>.
5. **Guo, Q.; Yu, T.; Jiang, D.** 2015. Robust H^∞ positional control of 2-DOF robotic arm driven by electro-hydraulic servo system, *ISA Transactions* 59: 55-64. <http://dx.doi.org/10.1016/j.isatra.2015.09.014>.
6. **Jia, Z.; Ma, J.; Wang, F.** 2011. Hybrid of simulated annealing and SVM for hydraulic valve characteristics prediction, *Expert Systems with Applications* 38: 8030-8036. <http://dx.doi.org/10.1016/j.eswa.2010.12.132>.
7. **Camacho, E. F.; Ramírez, D. R.; Limón, D.** 2010. Model predictive control techniques for hybrid systems, *Annual reviews in control* 34: 21-31. <https://doi.org/10.1016/j.arcontrol.2010.02.002>.
8. **Ayalew, B.; Jablolkow, K. W.** 2007. Partial feedback linearising force-tracking control: implementation and testing in electrohydraulic actuation, *Control Theory & Applications* 1: 689-698. <https://doi.org/10.1049/iet-cta:20060186>.
9. **Seo, J.; Venugopal, R.; Kenné, J. P.** 2007. Feedback linearization based control of a rotational hydraulic drive, *Control Engineering Practice* 15: 1495-1507. <https://doi.org/10.1016/j.conengprac.2007.02.009>.
10. **Zinober, A. S. I.; Liu, G., Shtessel, Y. B.** 2007. Sliding-mode control in systems with output time delay. *Mathematical Methods for Robust and Nonlinear Control, Lecture notes in control & information sciences* 367: 243-264. https://doi.org/10.1007/978-1-84800-025-4_9.
11. **Feki, M.** 2009. Sliding mode control and synchronization of chaotic systems with parametric uncertainties. *Chaos, Solitons & Fractals* 41: 1390-1400.

- <https://doi.org/10.1016/j.chaos.2008.05.022>.
12. **Kalsi, K.; Lian, J.; Hui, S.** 2010. Sliding-mode observers for systems with unknown inputs: A high-gain approach, *Automatica* 46: 347-353. <https://doi.org/10.1016/j.automatica.2009.10.040>.
 13. **Xiao, L. F.; Lu, B. B.; Yu, B.; Ye, Z. F.** 2015. Cascaded sliding mode force control for a single-rod electrohydraulic actuator, *Neurocomputin* 156: 117-120. <https://doi.org/10.1016/j.neucom.2014.12.078>.
 14. **Kyong, K. A.; Nguyen, H. T.** 2007. Design of a robust force controller for the new mini motion package using quantitative feedback theory, *Mechatronics* 17:542-550. <https://doi.org/10.1016/j.mechatronics.2007.07.011>.
 15. **Shao, P. Z.; Fang, Y. M.; Wang, W. B.; Jiao, Z. X.** 2012. Adaptive backstepping control of multi-model switching for the hydraulic servo position system of a rolling mill, *Beijing Keji Daxue Xuebao/Journal of University of Science and Technology Beijing* 34: 1346-1351.
 16. **Yang, J. H.; Li, S. Y.; Dai, Y. F.** 2006. Research on robust control strategy of valve controlled asymmetric cylinder position servo system, *Machine Tool & Hydraulics* 18: 2801-2805.
 17. **Jeyasenthil, R.; Choi, S. B.; Purohit, H.** 2019. Robust position control and disturbance rejection of an industrial plant emulator system using the feedforward-feedback control, *Mechatronic* 57: 29-38. <https://doi.org/10.1016/j.mechatronics.2018.11.004>.
 18. **Zhang, F.** 2005. Adaptive compensation of hydraulic servo control system, *Chinese Journal of Mechanical Engineering* 05: 94-97. <http://dx.doi.org/10.3901/JME.2005.05.094>.
 19. **Bo, Y.; Quan, L.** 2010. Control strategy of the electro-hydraulic position and speed hybrid servo system, *Journal of Mechanical Engineering* 24: 150-155. <http://dx.doi.org/10.3901/JME.2010.24.150>. <http://dx.doi.org/10.1016/j.mechatronics.2018.11.004>.
 20. **Eryilmaz, B.; Wilson, B. H.** 2006. Unified modeling and analysis of a proportional valve, *Journal of the Franklin Institute* 343(1): 48-68. <http://dx.doi.org/10.1016/j.jfranklin.2005.07.001>.
 21. **Fallahi, M.; Zareinejad, M.; Baghestan, K.; et al.** 2018. Precise position control of an electro-hydraulic servo system via robust linear approximation, *ISA Transactions* 80: 503-512. <https://doi.org/10.1016/j.isatra.2018.06.002>.
 22. **Ramamurthi, K.; Nandakumar, K.** 1999. Characteristics of flow through small sharp-edged cylindrical orifices, *Flow Measurement and Instrumentation* 10(3): 133-143. [http://dx.doi.org/10.1016/s0955-5986\(99\)00005-9](http://dx.doi.org/10.1016/s0955-5986(99)00005-9).
 23. **Zeng, L.; Yang, J.; Tan, J. P.** 2017. Compensation control of a non-zero open valve controlled asymmetric cylinder system based on model invariance, *Journal of Huazhong University of Science and Technology (Natural Science Edition)* 45: 29-34. <http://dx.doi.org/10.13245/j.hust.170305>.
 24. **Ferreira J. A.; Almeida Fernando Gomes De; Quintas Manuel Rodrigues.** 2002. A Semi-Empirical Model for a Hydraulic Servo-Solenoid Valve 216: 237-248. <https://doi.org/10.1243/095965102320005409>.
 25. **Steinboeck, A.; Kemmetmüller, W.; Lassel, C.; Kugi, A.** 2013. Model-based condition monitoring of an electro-hydraulic valve. *Journal of dynamic systems, Measurement and Control* 135: 061010-061010. <https://doi.org/10.1115/1.4024800>.
 26. **Borutzky, W.; Barnard, B.; Thoma, J.** 2002. An orifice flow model for laminar and turbulent conditions. *Simulation Modelling, Practice and Theory* 10(3-4): 141-152. [http://dx.doi.org/10.1016/S1569-190X\(02\)00092-8](http://dx.doi.org/10.1016/S1569-190X(02)00092-8).
 27. **Pan, X.; Wang, G.; Lu, Z.** 2011. Flow field simulation and a flow model of servo-valve spool valve orifice, *Energy Conversion and Management* 52(10): 3249-3256. <http://dx.doi.org/10.1016/j.enconman.2011.05.010>.
 28. **Merritt, H. E.** 1976. *Hydraulic Control Systems*. Wiley & Sons.
 29. **Ji, H.; Zhang, J.; Wang, D.** 2010. Flow coefficient of rectangular notch throttle orifice in spool valve, *Journal of Lanzhou University of Technology* 36(03): 47-50. <http://dx.doi.org/10.1360/972009-1551>.
 30. **Kumar, B.; Mittal, S.** 2006. Prediction of the critical Reynolds number for flow past a circular cylinder, *Computer Methods in Applied Mechanics & Engineering* 195: 44-47. <http://dx.doi.org/10.1016/j.cma.2005.10.009>.

L. Zeng, J. Yang, J. Tan

A COMPENSATOR DESIGNED FOR ELECTRO-HYDRAULIC SERVO SYSTEM IN LAMINAR STATE

S u m m a r y

The study researched the orifice flow equation when the flow state of the orifice is laminar. Based on the novel flow equation and the expected linear flow equation, a compensator is designed to compensate the non-linearity and make the flow characteristics linear. The characteristics experiment result shows that the flow after compensation control is close to the expected flow, in which the pressure difference was increased from 0.5MPa to 4MPa, and the error is less than 20%. When the compensator is used as feed forward control in the EHSS and compound with proportional (P) control, the sinusoidal response error with frequency of 0.5Hz and amplitude of 5mm is within 0.4mm under large external load. While the error of the uncompensated system is up to 0.8mm. The compensator can be used into the electro-hydraulic system with larger load disturbance and improve the control performance compounded with the simplest proportional (P) controller.

Keywords: laminar state, pressure difference, electro-hydraulic servo system, flow characteristics, feed forward control, compound control.

Received May 11, 2020
Accepted April 07, 2021

